Tunable superconductivity in parent cuprate $Pr_2CuO_{4\pm\delta}$ thin films

Xinjian Wei,[1,2] Ge He,[1,2] Wei Hu,[1,2] Xu Zhang,[1,2] Mingyang Qin,[1,2] Jie Yuan,[1] Beiyi Zhu,[1] Yuan Lin,[3] and Kui Jin[1,2,4,*]

[1]*Beijing National Laboratory for Condensed Matter Physics,*
Institute of Physics, Chinese Academy of Sciences, Beijing 100190, China
[2]*School of Physical Sciences, University of Chinese Academy of Sciences, Beijing 100049, China*
[3]*State Key Laboratory of Electronic Thin Films and Integrated Devices & Center for Information in Medicine,*
University of Electronic Science and Technology of China, Chengdu 610054, China
[4]*Collaborative Innovation Center of Quantum Matter, Beijing 100190, China*
(Dated: July 4, 2018)

In this article, we studied the role of oxygen in $Pr_2CuO_{4\pm\delta}$ thin films fabricated by polymer assisted deposition method. The magnetoresistance and Hall resistivity of $Pr_2CuO_{4\pm\delta}$ samples were systematically investigated. It is found that with decreasing the oxygen content, the low-temperature Hall coefficient (R_H) and magnetoresistance change from negative to positive, similar to those with the increase of Ce-doped concentration in $R_{2-x}Ce_xCuO_4$ (R= La, Nd, Pr, Sm, Eu). In addition, T_c versus R_H for both $Pr_{2-x}Ce_xCuO_4$ and $Pr_2CuO_{4\pm\delta}$ samples can coincide with each other. We conclude that the doped electrons induced by the oxygen removal are responsible for the superconductivity of T'-phase parent compounds.

PACS numbers: 74.72.Ek, 81.15.-z, 73.50.-h,

I. INTRODUCTION

Studying parent compounds of high-T_c superconductors is crucial to unveiling the mechanism of high-temperature superconductivity, as well as provides significant clues to explore new superconductors. Parent compounds of the cuprates have been long considered as antiferromagnetic Mott insulators, which can be tuned to superconductors by doping holes or electrons[1]. For example, Sr^{2+} cations substitutes La^{3+} cations in hole-doped $La_{2-x}Sr_xCuO_4$ or Ce^{4+} cations substitutes R^{3+} cations in electron-doped $R_{2-x}Ce_xCuO_4$ (R= La, Nd, Pr, Sm, Eu)[2]. Besides the Ce-doped concentration, superconductivity of the electron-doped cuprates depends heavily on the oxygen content. In 1995, T_c of the underdoped $Pr_{2-x}Ce_xCuO_4$ (PCCO) by the protected annealing was enhanced comparable to that of the optimally doped one[3]. In 2008, the superconductivity in parent thin films T'-R_2CuO_4 (R= Nd, Pr, Sm, Eu, Gd) was achieved by low-temperature annealing under the high-vacuum environment[4]. This momentous discovery seemingly challenges the commonly accepted model that high-T_c superconductivity results from doping extra carriers into Mott insulators.

However, the intrinsic physics of superconductivity in the parent compounds is still under debate. Optical conductivity measurements on $Pr_2CuO_{4\pm\delta}$ (PCO) thin films have disclosed that the AFM-correlated "pseudogap" does not exist in this system, which indicates that the T'-phase parent cuprates are metallic and superconductivity occurs at low temperature[5]. In fact, it is impossible to avoid oxygen defects during the sample preparation, which can introduce extra carriers into CuO_2 planes and lead to superconductivity. Wei *et al.*[6] found that the superconducting T'-La_2CuO_4 thin film can be tuned into an insulator by substituting Sr^{2+} for La^{3+}.

They suggest that T'-phase parent cuprates are Mott insulators, while the intrinsic defects, most likely oxygen vacancies, are the sources of the effective carriers in these materials. Moreover, dynamical mean field theory (DMFT) studies demonstrate that the parent compounds may be described as weakly correlated Slater insulators rather than the strongly correlated charge transfer insulators[7,8]. Electrical transport measurement is a common but powerful method to explore the intrinsic electronic state in various superconductors. Plenty of studies in $R_{2-x}Ce_xCuO_4$ materials[9–13] support that the negative magnetoresistance (MR) and nonlinear magnetic field dependence of Hall resistivity are associated with antiferromagnetic order, Fermi surface reconstruction, quantum phase transition etc., which take a significant role in understanding the mechanism of high-T_c superconductivity. Nevertheless, the systematic electrical transport investigations have been seldom addressed in parent system.

In this paper, we carried out systematical MR and Hall resistivity measurements on the superconducting PCO thin films which were synthesized on $SrTiO_3$ (STO) substrates by polymer assisted deposition method. With the decrease of oxygen content, the low-temperature MR gradually changes from negative to positive. Meanwhile, the low-temperature Hall coefficient R_H undergo a sign reversal, suggesting that dominant carriers vary from electrons to holes. All the behaviors are quite similar to those in $R_{2-x}Ce_xCuO_4$ materials. Furthermore, we plotted the T_c versus R_H for both PCCO and PCO samples, and found that their evolution could coincide with each other. Our results imply that the carriers induced by the oxygen removal benefit the superconductivity in T'-parent cuprates.

II. PREPARATION AND MEASUREMENTS

Till now, the superconducting parent compounds have been successfully synthesized by metal-organic decomposition (MOD)[4] and molecular beam epitaxy (MBE) methods[6,14,15]. In general, high-purity naphthenates used in MOD are extremely rare and expensive. Alternatively, MBE facility is very expensive, and it is of low-efficiency during the thin film preparation. Therefore, to develop a high-efficiency and inexpensive method is necessary for preparing the superconducting parent thin films. Polymer assisted deposition (PAD) is a newly developed method in recent years, which has the advantages of easy operation, low cost and stable precursor solutions[16,17]. Fig. 1(a) is a schematic diagram of PAD method. First, metal ions are electrostatically bound to the polymer in deionized water, forming a uniform and stable solution. Second, the solution is applied onto a substrate through either spin-coating or dipping. Finally the coated substrate is treated at a desired temperature in an oxygen environment to remove the polymer and enable the growth of the metal-oxide film.
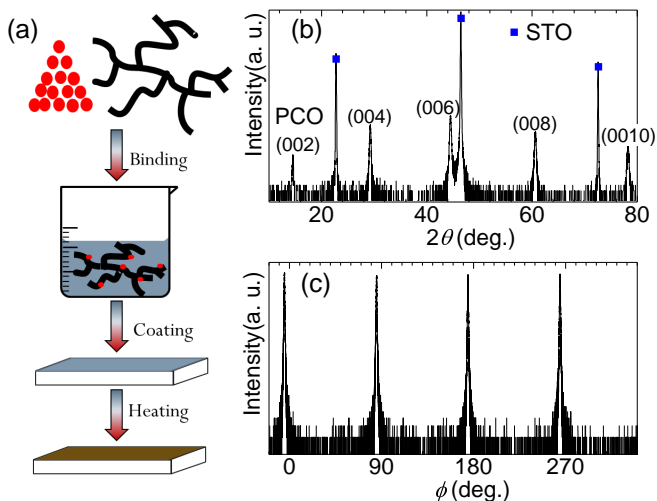

FIG. 1. (Color online) (a) The schematic diagram of polymer assisted deposition method. (b), (c) XRD 2θ-scans and ϕ-scan of the $Pr_2CuO_{4\pm\delta}$ film on the $SrTiO_3$ (001) substrate.

To prepare high-quality superconducting PCO thin films, the metal ion sources are Pr and Cu nitrates, and the organic compounds are polyethylenimine (PEI) and ethylenediaminetetraacetic acid (EDTA). The concentration of Pr (Cu) metal ions in the solution was determined by inductively coupled plasma-atomic emission spectroscopy measurement. Then the precursor solution was obtained by mixing Pr solution and Cu solution at a certain stoichiometric ratio. In order to prevent the Cu absence, we made the precursor solution with 50% Cu overdose. The precursor solution was spin coated on STO substrates. The polymer was pyrolyzed by heating gradually from the room temperature to 550 °C in the air. After that samples were sintered and crystallized at 850 °C for one hour in a tubular furnace under the oxygen pressure about 200 Pa. Finally the films were annealed in low-oxygen pressure about 1 Pa at various temperatures.
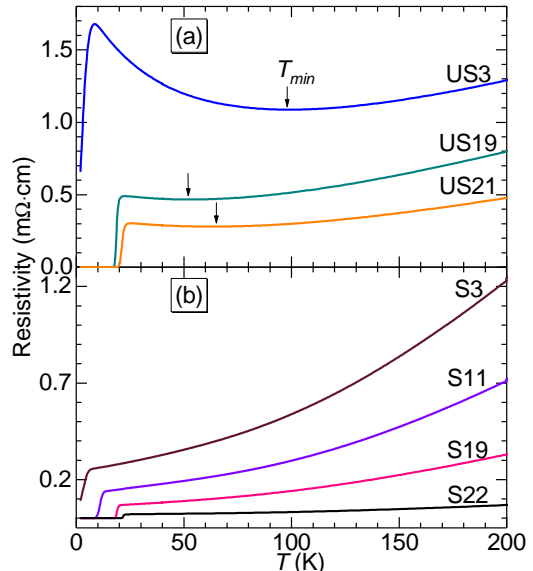

FIG. 2. (Color online) Resistivity as a function of temperature for $Pr_2CuO_{4\pm\delta}$ films with various oxygen content. (a) The resistivity of US3, US19 and US21 shows an upturn at the temperature defined as T_{min}. (b) Resistivity versus temperature of S22, S19, S11 and S3 samples shows a good metallic behavior. The number in the sample name presents the superconducting transition temperature.

To characterize the structure and crystalline of PCO thin films, we measured the $\theta/2\theta$ and ϕ-scan of the samples using x-ray diffractometer. The XRD 2θ-scan of the PCO film on STO (001) is shown in Fig. 1(b). All peaks are sharp and can be indexed to (00l) of the T'-structure, indicating that the film shows a single phase and c-axis orientation. Fig. 1(c) exhibits ϕ-scan data with the approximately equal peak intensities, meaning that sample has a good epitaxy. Subsequently, electrical transport properties were measured by a 9 T physical property measurement system. In order to improve the measurement accuracy, all samples were patterned into standard Hall bridge. The range of the magnetic field is -9∼9 T which was perpendicular to the film surface during the MR and Hall resistivity measurements.

III. RESULTS AND DISCUSSIONS

In Fig. 2, we present the temperature dependence of the resistivity for various PCO thin films. With the decrease of the temperature, resistivity for US3, US21 and US19 samples shows an upturn at the temperature T_{min}. Considering that c_0 should have a positive correlation with the relative oxygen content of the samples[18], we calculated the c-axis lattice constants c_0 of PCO films (see

TABLE I. Summary of the transport properties and lattice structure constant c_0 of PCO films. T_c is the superconducting transition temperature where the resistance becomes a half of the normal state value. T_0 represents the transition temperature of MR from negative to positive of US3, US21 and US19 samples. RRR is the resistance ratio of $R(300\text{ K})/R(30\text{ K})$. c_0 is the c-axis lattice constant.

Number	T_c(K)	T_{min}(K)	T_0(K)	c_0(Å)	RRR
US3	2.5	98	105 ± 5	12.213	1.2
US21	21.2	65	75 ± 5	12.212	2.5
US19	18.7	52	55 ± 5	12.211	2.4
S22	21.9			12.205	4.8
S19	18.9			12.202	7.8
S11	11.0			12.201	8.0
S3	2.7			12.199	7.2

Table I) by Bragg diffraction formula from the XRD data. It is worth mentioning that T_{min} gradually decrease as the c_0 reduces and the upturn behavior disappears for S22, S19, S11 and S3.
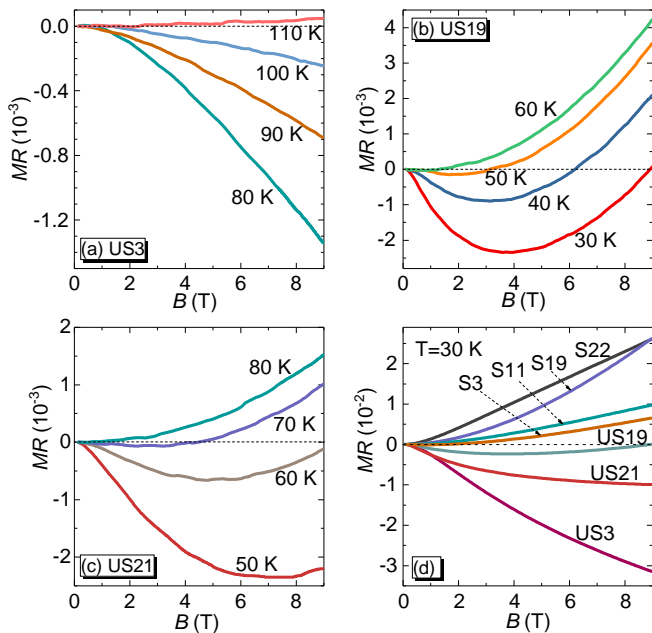

FIG. 3. (Color online) (a), (b), (c) MR versus magnetic field B for US3, US19 and US21, respectively. (d) MR curves for the various $Pr_2CuO_{4+\delta}$ films at T=30 K.

In the underdoped region of Ce-doped cuprates, the low-temperature resistivity also shows an upturn which gradually disappears with the increase of Ce concentration[11,19]. High magnetic field can suppress this upturn behavior, resulting in a negative MR[13]. Fig. 3 displays the field dependence of MR, with applied field parallel to the c-axis ($B//c$). The MRs of US3, US21 and US19 samples are negative at the low temperature and turn into positive at the high temperature as shown in Fig.3 (a), (b) and (c). We define the transition temperature as T_0 which performs a consistent tendency with

T_{min} (as shown in Table I). Besides, the low-temperature negative MR fades away as reducing the oxygen content(Fig. 3(d)). We conjecture that the mechanisms of the upturn and negative MR in US3, US21 and US19 samples are the same as those in the under-doped region of Ce-doped cuprates.

The Hall coefficient R_H can illuminate the nature of material carriers. For example, the low-temperature R_H in the $R_{2-x}Ce_xCuO_4$ system varies from negative to positive as the Ce-doped concentration increases, corresponding to the carriers varying from electrons to holes[9,12,20]. Fig. 4(a) exhibits R_H as a function of temperature for various samples. The R_Hs of US3, US19 and US21 are negative in the whole temperature range, suggesting that the electron is predominant in the transport process. The sign reversal of R_H arises in S22 and S19 as the temperature increases, i.e. from positive to negative, which reveals a competition between electron and hole carriers. The R_Hs of S11 and S3 are positive below 150 K, indicating that the dominant carriers are holes.
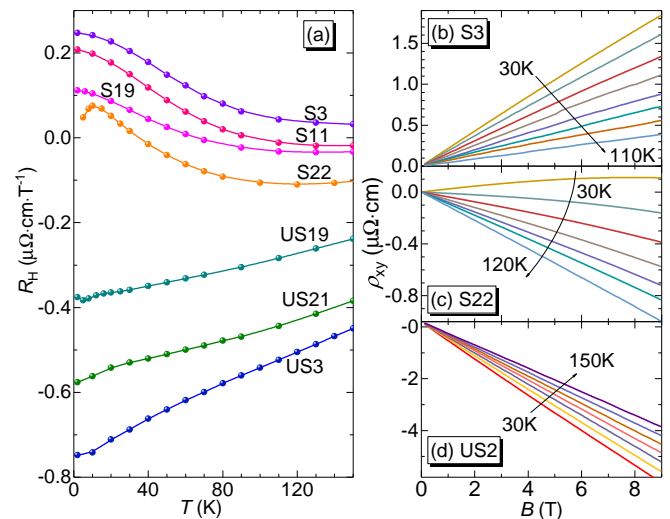

FIG. 4. (Color online) (a) Normal state Hall coefficient R_H versus temperature for $Pr_2CuO_{4+\delta}$ films measured at B=9 T ($B//c$). (b), (c), (d) Hall resistivity ρ_{xy} versus B for S3, S22, US3.

Fig. 4(b), (c) and (d) display the Hall resistivity ρ_{xy} at various temperature for US3, S22 and S3, respectively. For US3 and S3, the ρ_{xy} as a function of magnetic field exhibits a good linear behavior, indicating that the samples have a single band characteristic. The low-temperature ρ_{xy} of S22 sample is nonlinear to the magnetic field, which implies the coexistence of electron and hole band. For Ce-doped cuprates, Fermi surface of the optimum doped samples is reconstructed by antiferromagnetic order[12,21,22]. Therefore, we can surmise that Fermi surface of the parent compounds can be gradually adjusted by changing the oxygen content.

As mentioned above, it can be concluded that, for MR and Hall resistivity, the effects of varying oxygen content in PCO thin films are similar to that of varying Ce con-

centration in PCCO. Such phenomenon indicates that the oxygen removal can induce carrier doping. This finding seemingly supports the scenario that superconductivity in parent compounds is obtained via doping a Mott insulator, symmetric to the hole-doped side. We note that this view has been clarified in the recent ARPES results as well[6,23].

Unfortunately, it is extremely difficult to measure the accurate oxygen content which also plays a non-ignorable role in $R_{2-x}Ce_xCuO_4$. Song *et al.*[24] studied $Pr_{1-x}LaCe_xCuO_4$ samples with different Ce concentrations and annealing processes using ARPES. They found that effective electron number estimated from Fermi surface volume could unify the effect of Ce doping and deoxygenation. For electrical transports, R_H is the most qualified quantity reflecting the information of carriers. Therefore, we try to set R_H as the horizontal axis to study the evolution of T_c in both PCCO and PCO systems. As shown in Fig. 5, we find that all the data from distinct groups, various measuring conditions and different samples obey the same rule, i.e. T_c increases at first and then decreases as R_H increases. Especially, T_c always reaches its maximum near $R_H = 0$, which indicates that the balance between the electron and hole bands is beneficial to the superconductivity of electron-doped cuprates, consistent with the electrostatic tuning results of $Pr_{1.85}Ce_{0.15}CuO_4$[25].
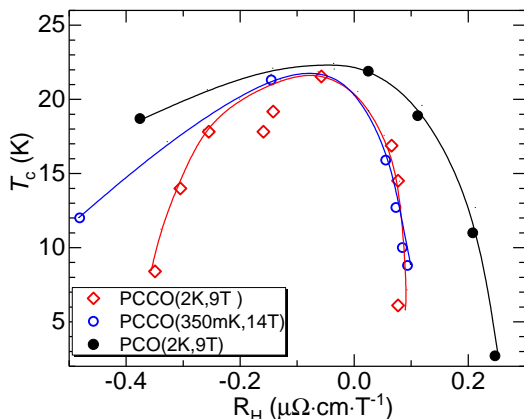

FIG. 5. (Color online) T_c versus R_H of both PCO and PCCO. PCCO (2 K, 9 T) and PCCO (340 mK, 14 T) data derive from ref. 12 and ref. 20 respectively. The solid curve is a guide to the eye.

For the underdoped PCCO samples, the R_H rapidly decreases as temperature decreases, independent of the magnetic field[12,26]. Therefore, the clear difference between two group data of PCCO is mainly attributed to the temperature distinction. Of obviously, we cannot ex-

clude the influence of antiferromagnetic order and disorder. The PCCO data show a perfect overlap in the overdoped region because the R_H is hardly dependent on the temperature and linear with magnetic filed in this region. As shown in Fig. 5, we can see that the T_c of PCO is always greater than that of PCCO samples at a fixed R_H value. This can be explained as the following. In PCO and PCCO, the change in T_c is mainly due to the change of carrier concentration and structural disorder i.e. $\Delta T_c = \Delta T_c(R_H) + \Delta T_c(\text{disorder})$. We assume that the $\Delta T_c(R_H)$ induced by Ce doping or oxygen changes is identical for both PCO and PCCO samples. The disorder in PCCO is caused by Ce doping and O content changes. In contrast, the disorder in PCO can be just attributed to changing the oxygen content. So the absolute $\Delta T_c(\text{disorder})$ of PCO is less than that of PCCO at a fixed R_H value. This suggests the disorder introduced by Ce doping is more than that by deoxygenation. It can be understood by that Ce doping causes a structure distortion and brings more disorder in PCCO. This finding can explain why T_c in the parent compounds are even higher than that of the optimal Ce-doped samples[18] and also support that the superconductivity in T'-phase parent cuprates stems from doping effect induced by the oxygen removal.

In summary, a series of high-quality superconducting PCO thin films have been prepared by polymer assisted deposition method. The magnetoresistance and Hall effect of superconducting PCO thin films with various oxygen content are systematically studied. It is found that for the magnetoresistance and Hall resistivity, the effect of oxygen removal in PCO is similar to that of the Ce doping in $R_{2-x}Ce_xCuO_4$. In addition, we find that Hall coefficient R_H is an efficient parameter to depict the evolution of T_c in the electron-doped cuprates. We argue that doped electrons induced by the oxygen removal are the cause of the superconductivity in T'-parent compounds.

IV. ACKNOWLEDGMENTS

* kuijin@iphy.ac.cn

[1] P. A. Lee, N. Nagaosa, and X. G. Wen, Rev. Mod. Phys. **78**, 17 (2006).

[2] N. P. Armitage, P. Fournier, and R. L. Greene, Rev. Mod. Phys. **82**, 2421 (2010).

[3] M. Brinkmann, T. Rex, H. Bach, and K. Westerholt, Phys. Rev. Lett. **74**, 4927 (1995).

[4] O. Matsumoto, A. Utsuki, A. Tsukada, H. Yamamoto, T. Manabe, and M. Naito, Physica C **468**, 1148 (2008).

[5] G. Chanda, R. P. S. M. Lobo, E. Schachinger, J. Wosnitza, M. Naito, and A. V. Pronin, Phy. Rev. B **90**, 024503 (2014).

[6] H. I. Wei, C. Adamo, E. A. Nowadnick, E. B. Lochocki, S. Chatterjee, J. P. Ruf, M. R. Beasley, D. G. Schlom, and K. M. Shen, Phys. Rev. Lett. **117**, 147002 (2016).

[7] C. Weber, K. Haule, and G. Kotliar, Nat. Phys. **6**, 574 (2010).

[8] C. Weber, K. Haule, and G. Kotliar, Phys. Rev. B **82**, 125107 (2010).

[9] K. Jin, X. H. Zhang, P. Bach, and R. L. Greene, Phys. Rev. B **80**, 012501 (2009).

[10] K. Jin, N. P. Butch, K. Kirshenbaum, J. Paglione, and R. L. Greene, Nature **476**, 73 (2011).

[11] Y. Dagan, M. C. Barr, W. M. Fisher, R. Beck, T. Dhakal, A. Biswas, and R. L. Greene, Phys. Rev. Lett. **94**, 057005 (2005).

[12] Y. Dagan, M. M. Qazilbash, C. P. Hill, V. N. Kulkarni, and R. L. Greene, Phys. Rev. Lett. **92**, 167001 (2004).

[13] X. Zhang, H. S. Yu, G. He, W. Hu, J. Yuan, B. Y. Zhu, and K. Jin, Physica C **525**, 18 (2016).

[14] H. Yamamoto, O. Matsumoto, A. Tsukada, and M. Naito, Physica C **470**, 1025 (2010).

[15] H. Yamamoto, O. Matsumoto, Y. Krockenberger, K. Yamagami, and M. Naito, Solid State Commun. **151**, 771 (2011).

[16] Q. X. Jia, T. M. McCleskey, A. K. Burrell, Y. Lin, G. E. Collis, H. Wang, A. D. Li, and S. R. Foltyn, Nat. Mater. **3**, 529 (2004).

[17] A. K. Burrell, T. Mark McCleskey, and Q. X. Jia, Chem. Commun. (Camb) , 1271 (2008).

[18] O. Matsumoto, A. Utsuki, A. Tsukada, H. Yamamoto, T. Manabe, and M. Naito, Phys. Rev. B **79**, 100508 (2009).

[19] S. Finkelman, M. Sachs, G. Droulers, N. P. Butch, J. Paglione, P. Bach, R. L. Greene, and Y. Dagan, Phys. Rev. B **82**, 094508 (2010).

[20] S. Charpentier, G. Roberge, S. Godin-Proulx, X. Bechamp-Laganiere, K. D. Truong, P. Fournier, and P. Rauwel, Phys. Rev. B **81**, 104509 (2010).

[21] J. Lin and A. J. Millis, Phys. Rev. B **72**, 214506 (2005).

[22] T. Sarkar, P. R. Mandal, J. S. Higgins, Y. Zhao, H. Yu, K. Jin, and R. L. Greene, Phys. Rev. B **96**, 155449 (2017).

[23] M. Horio, Y. Krockenberger, K. Koshiishi, S. Nakata, K. Hagiwara, M. Kobayashi, K. Horiba, H. Kumigashira, H. Irie, and H. Yamamoto, arXiv:1801.03702.

[24] D. Song, G. Han, W. Kyung, J. Seo, S. Cho, B. S. Kim, M. Arita, K. Shimada, H. Namatame, M. Taniguchi, Y. Yoshida, H. Eisaki, S. R. Park, and C. Kim, Phys. Rev. Lett. **118**, 137001 (2017).

[25] K. Jin, W. Hu, B. Zhu, D. Kim, J. Yuan, Y. Sun, T. Xiang, M. S. Fuhrer, I. Takeuchi, and R. L. Greene, Sci. Rep. **6**, 26642 (2016).

[26] P. Li, F. F. Balakirev, and R. L. Greene, Phys. Rev. Lett. **99**, 047003 (2007).